Available online at www.sciencedirect.com

ScienceDirect

Underground Space 26 (2026) 321–340

www.keaipublishing.com/undsp

Research Paper

Incorporating smart computer vision and in-drilling information into rock quality evaluation via incomplete data-driven Bayesian networks

Chen Wu [a], Minglun Tan [b], Yue Tong [c], Hongwei Huang [a,*]

[a] Department of Geotechnical Engineering, Tongji University, Shanghai 200092, China
[b] Qingdao Guoxin Jiaozhou Bay Second Submarine Tunnel Co., Ltd., Qingdao 266000, China
[c] Yunan Communications Investment & Construction Group Co., Ltd., Kunming 650228, China

Received 11 August 2024; received in revised form 24 January 2025; accepted 4 March 2025
Available online 15 October 2025

Abstract

Tunnelling is a challenging task due to a lack of full understanding of the surrounding rock quality. This study proposes a solution driven by a refined computer vision (CV) method, complemented by rock mass drilling tests and Bayesian networks, to address this issue through a multi-source heterogeneous data approach. Initially, improvements are made to the popular Swin Transformer to improve the recognition and segmentation of intricate rock features. Notably, refined smart CV, owing to its U-shaped architecture and smart window self-attention computation, exhibits segmentation performance superior to that of conventional CV methods such as Swin Transformer, Deeplab V3+, and UNet. Building upon the segmentation outcomes of the refined CV, a parameter set comprising apparent rock parameters is established. Then, two datasets encompassing rock internal drilling parameters and mechanics, as well as design parameters, are curated. The combination of the aforementioned parameter sets is referred to as the rock quality comprehensive evaluation dataset. However, analysis reveals data incompleteness issues within these datasets. To mitigate this problem, a novel tree-augmented Bayesian network is designed, and a prediction accuracy of 91% is realized, surpassing popular decision trees, ensemble learning, and deep learning methods. Furthermore, evaluation services are provided in mountain and submarine tunnels, suggesting that drilling parameters significantly enhance the evaluation performance. Moreover, employing two sensitivity analysis metrics underscores the prominent influence of rotating pressure and drilling speed parameters. This study endeavor presents diverse solutions for achieving precise and expeditious predictions of rock quality through various parameter sets, tailored to cater to diverse requirements of tunnels.

Keywords: Rock mass quality; Smart computer vision; Drilling parameters; Incomplete datasets; Tree augmented naive Bayesian

1 Introduction

The evaluation of surrounding rock quality at tunnel faces represents a pivotal phase in tunnel design and construction employing the New Austrian Tunnelling Method, forming the bedrock for scientifically designing tunnel support and ensuring the smooth implementation of construction activities (Chen & Liu, 2007; Ismail et al., 2019; Tu et al., 2019). Presently, prevalent methods for assessing rock mass quality predominantly revolve around established metrics such as rock quality designation, the quality system (Barton et al., 1974), rock mass rating (RMR) system, and rock mass index (Palmstrom, 1996). While there exists a consensus on the adoption of qualitative and quantitative multifactorial classification methods for selecting evaluation parameters (e.g., rock strength, rock mass integrity, groundwater conditions, etc.), variations persist in parameter weighting, representation modalities, and the grading of rock quality. Moreover, the acquisition of these parameters heavily depends on manual expertise and lacks

* Corresponding author at: Department of Geotechnical Engineering, Tongji University, Shanghai 200092, China.
E-mail address: huanghw@tongji.edu.cn (H. Huang).
Peer review under the responsibility of Tongji University

https://doi.org/10.1016/j.undsp.2025.03.007

automation. Existing methods mainly focus on apparent rock parameters, overlooking internal parameters such as internal integrity, internal fractures, and the extent of water seepage, even though these parameters can now be obtained through drilling and other means (S. Li et al., 2017; Yue et al., 2004). This constraint hinders further enhancement of evaluation performance. Hence, the continued advancement of more accurate and intelligent methods for evaluating rock quality holds significance and merits attention and effort from tunneling experts and scholars globally (Chen et al., 2017; Hou et al., 2022; Zhou et al., 2021).

The evaluation of rock quality necessitates the direct measurement and recording of critical parameters, including rock strength, groundwater, joint spacing, and the presence of weak interlayers directly at the tunnel face. However, conducting these evaluations manually in front of the tunnel face poses inherent safety risks and can be subject to variations based on the expertise and experience of the engineer, potentially leading to inaccuracies in prediction. In response to these challenges, non-contact computer vision (CV) methodologies have garnered considerable attention among tunnel experts and engineers for evaluating rock parameters (Chen et al., 2021a; Huang et al., 2021). CV approaches offer a safer, expedited, and more objective alternative to traditional manual assessments (Patel & Chatterjee, 2016). Despite these advantages, CV-based identification strategies encounter notable challenges due to the intricate nature of fractures, groundwater, weak interlayers, and the diverse image backgrounds encountered at tunnel faces. The majority of CV models applied to rock feature analysis are adaptations of generic CV architectures such as convolutional neural networks (CNN) and Transformers, which have not been specifically tailored for the nuances of rock evaluation parameters. Consequently, the performance of CNN and Transformer-based models in intelligently extracting these parameters is somewhat limited (J. Chen et al., 2022; Wu et al., 2023). Thus, there exists a compelling exigency to refine CV models for the precise identification of minuscule and complex boundary parameters, thereby enhancing their capacity to intelligently identify interlayers, groundwater features, and fractures. These advancements carry profound implications for engineering practice.

Numerous researchers have conducted extensive studies on the evaluation of rock quality utilizing CV methodologies. For instance, Zhou et al. (2021) utilized CV techniques to extract related evaluation parameters, including fractures and groundwater, to predict the rock quality. A CV model named FrasegNet and a deep learning (DL) method are employed by Chen et al. (2021a) to assess the state of joint fractures in rock. Nevertheless, these approaches mainly emphasize rock surface features, which can be susceptible to influences from drilling and blasting operations. Notably, the internal parameters that most accurately reflect overall rock quality have not been sufficiently integrated into these methodologies, potentially resulting in incomplete and inaccurate evaluations. To address these limitations, advanced horizontal drilling parameters-such as drilling speed, drilling pressure, and torque—that directly reflect the rock internal state should be incorporated alongside apparent parameters. This integrated approach will enable a more comprehensive evaluation, promising substantial enhancements in evaluation accuracy (S. Li et al., 2017; Wang et al., 2021).

Moreover, in the evaluation process, a multitude of evaluation parameters—such as groundwater, fractures, weak interlayers, mechanical properties, and design specifications—are typically taken into consideration by scholars and engineers (Guo et al., 2023; Zhou et al., 2021). Nonetheless, the challenges posed by confined spaces, limited illumination, and the compact nature of tunnel construction processes often hinder the acquisition of complete parameters concurrently. This limitation thereby curtails the efficacy of conventional methods commonly employed for predicting. Consequently, the task of predicting rock quality based on incomplete datasets needs significant consideration and attention. Bayesian network (BN) offer a viable approach for handling incomplete datasets, serving as a type of probabilistic graphical model that elucidates variable relationships through node connections (Feng & Jimenez, 2015). BNs can effectively learn parameters and structures from incomplete datasets, leveraging Bayesian theorem to predict unknown information using prior and posterior probabilities. Moreover, prior studies by Feng and Jimenez (2015) and N. Li et al. (2017b) have successfully demonstrated the applicability of BNs in predicting tunnel deformation and rock burst severity, respectively, utilizing incomplete datasets. Therefore, the utilization of BNs to forecast quality based on incomplete datasets holds substantial significance. Furthermore, within the domain of geotechnical engineering assessment tasks, Hou et al. (2022) applied a set of 10 characteristic parameters for real-time classification of rock masses, while N. Li et al (2017a) focused on utilizing 7 parameters to predict rock bursts. Despite their respective successes, these studies did not explore the impact of different parameter combinations on outcomes, nor did they address the inquiry regarding the potential correlation between the number of parameters and effectiveness.

In this investigation, a substantial volume of valuable in-situ drilling parameters pertaining to rock characteristics is acquired from tunnel sites. An improved CV model is employed to quantitatively identify rock features. Six evaluation parameter sets are developed, encompassing apparent, internal, mechanical, and design parameters. Leveraging the developed parameter sets and the newly designed BN, this study endeavors to achieve precise prediction through the implementation of diverse parameter sets, thereby offering tailored rock quality assessment services for tunnels characterized by different attributes. Further, it identifies the paramount parameters that exert the most profound influence on rock quality.

2 Methodology

The primary process for assessing rock quality is depicted in Fig. 1. This study mainly employs an improved CV model and a BN. The former is utilized to quantify the segmented rock features, while the latter is employed for data-driven evaluation based on the quantified features. Details of two methods are provided below.

2.1 Improving CV model

The Swin Transformer (Swin T) model (Fig. 2(a)), a CV model rooted in the Transformer architecture, has been extensively employed in visual tasks such as image segmentation within the field of underground engineering (Liu et al., 2021; Qin et al., 2024; Wu et al., 2023; Zhou et al., 2023). Embracing a stratified design and self-attention mechanisms, it achieves profound insights into image comprehension and representation. Its self-attention mechanism relies mainly on two sub-modules: window-based multi-head self-attention (W-MSA) and shifted W-MSA (SW-MSA). The W-MSA module primarily focuses on local information, capturing interactions between pixels within the defined window. In contrast, the SW-MSA module is oriented towards capturing global information. Despite its success, the model faces challenges in accurately identifying complex features such as water leakage and fractures (Chen et al., 2021a; Wu et al., 2023). Conversely, the UNet model has garnered substantial recognition for its prowess in discerning intricate features, and its basic structure is plotted in Fig. 2(b). To improve the efficacy of the Swin T in underground engineering, integrating the structural attributes of the UNet is being explored as a strategic enhancement.

The improved Swin T structure depicted in Fig. 3(a) consists of three key segments: the Encoding group, Skipping group, and Decoding group (Fu et al., 2024; Lin et al., 2022). Within the Encoding group are three smart Swin T modules, each integrating a W-MSA and a designed smart SW-MSA (SSW-MSA) module (Fu et al., 2024; Liu et al., 2021). Drawing inspiration from the UNet model's exceptional architecture for enabling information exchange between encoders and decoders, features from both these components are interconnected via foundational bridges and skip connections across various layers. Positioned on the left and right sides of the Skipping group are patch merging and patch expansion modules, respectively. The patch merging module effectively reduces feature map dimensions while augmenting channel capacity, thereby significantly boosting the model's sensitivity to rock features with minute details. The improved Swin T with SSW-MSA module is designated as the face rock features segmentation (FRFseg) model within this work. The FRFseg model, enhanced for image processing tasks, accepts input rock feature images. The image undergoes segmentation into multiple patches using a patch embedding module, followed by processing through the encoder. Within the W-MSA module in the smart Swin T, these patches are organized into windows for self-attention computation. The resultant output from W-MSA is then forwarded into SSW-MSA, leveraging a mechanism to enable cross-window interactions across different channels. Through the combined operations of W-MSA and SSW-MSA, the model effectively extracts high-fidelity local detail features alongside global representations. In the fusion stage, features from each encoder scale are seamlessly integrated with their corresponding decoder counterparts. Subsequently, feature dimension reduction is achieved via per-patch linear transformations, ensuring consistency with the subsequent module's input requirements.

For the SSW-MSA module in FRFseg, the masks applied to self-attention matrices remain uniform and

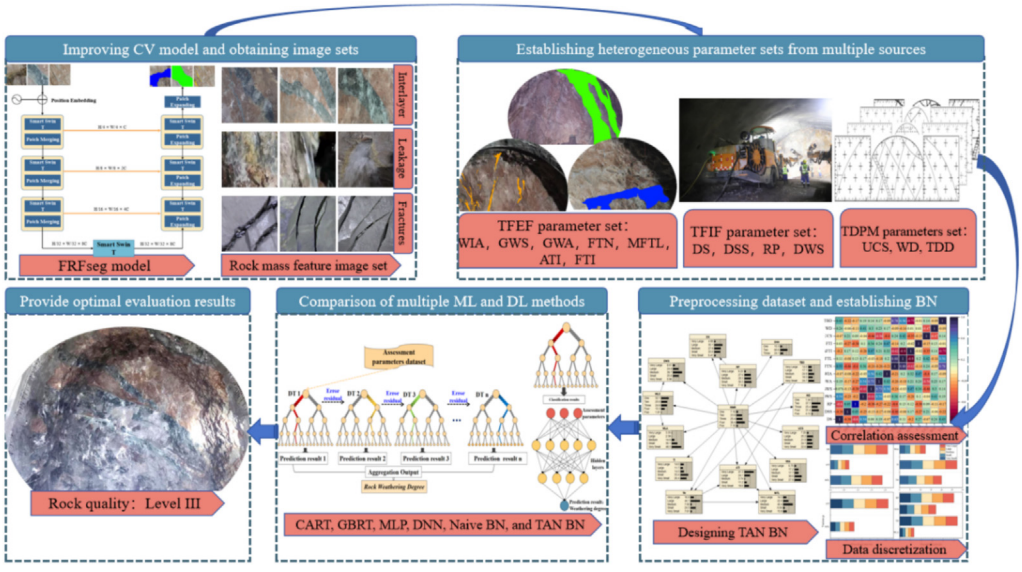

Fig. 1. Workflow of the tunnel rock mass quality evaluation.

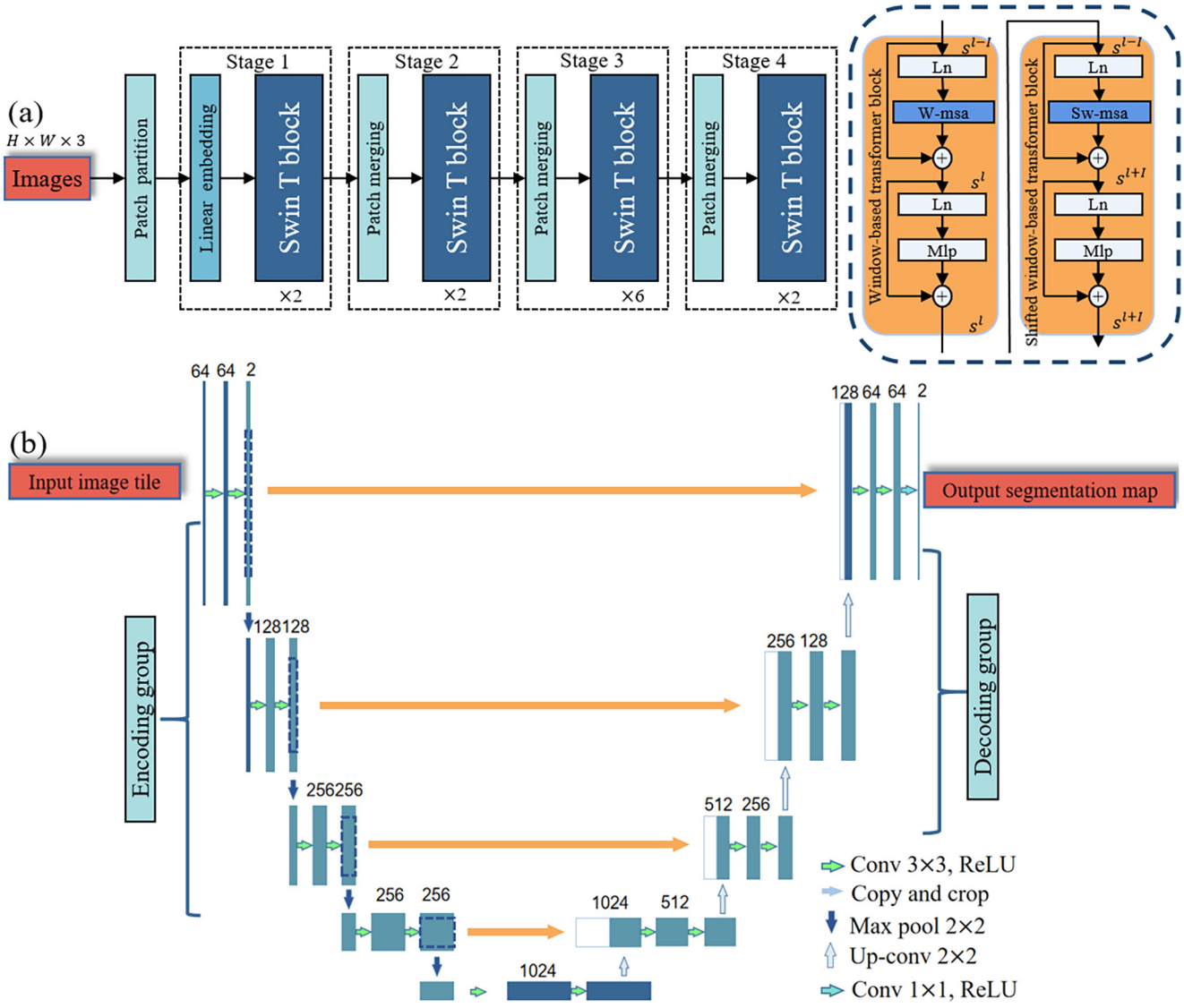

Fig. 2. Fundamental structures of (a) traditional Swin T and (b) UNet.

are employed to obscure fine-grained details pertaining to interactions between distant pixels. This uniform masking approach lacks nuanced channel-specific feature representations, neglecting the inherent variation in feature importance across different channels. To utilize the full potential of channel-specific characteristics, the FRFseg model adopts channel-adaptive masking, where masks for each channel are dynamically determined based on the channel's characteristics. This adaptive approach automatically learns which pixel interactions to preserve and which to obscure. The intelligent masks are depicted in Fig. 3(b). Notably, these intelligent masks mainly impact the self-attention matrices. The detailed formulation of the employed smart self-attention module is presented below (Fu et al., 2024):

$$\text{Self-Attention}\ (\boldsymbol{Q},\boldsymbol{K},\boldsymbol{V}) = \text{Softmax}\left(\frac{\boldsymbol{Q}\boldsymbol{K}^{\mathrm{T}}}{\sqrt{d}} + \text{Smart} - \text{Mask}\right)\boldsymbol{V}, \tag{1}$$

where $\boldsymbol{Q}$, $\boldsymbol{K}$, and $\boldsymbol{V}$ are the Query, Key, and Value matrices in the input, respectively, with d representing the dimensionality of $\boldsymbol{K}$ or $\boldsymbol{Q}$. This intelligent mask in SSW-MSA is of equivalent size to the self-attention matrix and produces varying masks within its channels. Notably, it undergoes automatic learning.

Compared to conventional fixed masks applied in Swin T, the intelligent mask demonstrates significant advantages by creating distinct masks across different channels to fully exploit channel functionalities. The SSW-MSA module notably enhances the recognition of complex detail features in the tunnel face by preserving accurate contextual information and removing irrelevant interactions. Furthermore, leveraging the local and global detail information provided by the W-MSA and SSW-MSA, the FRFseg effectively integrates multi-scale detail information, demonstrating superior information acquisition capabilities, particularly in representing complex detail features such as interlayers and joint fissures.

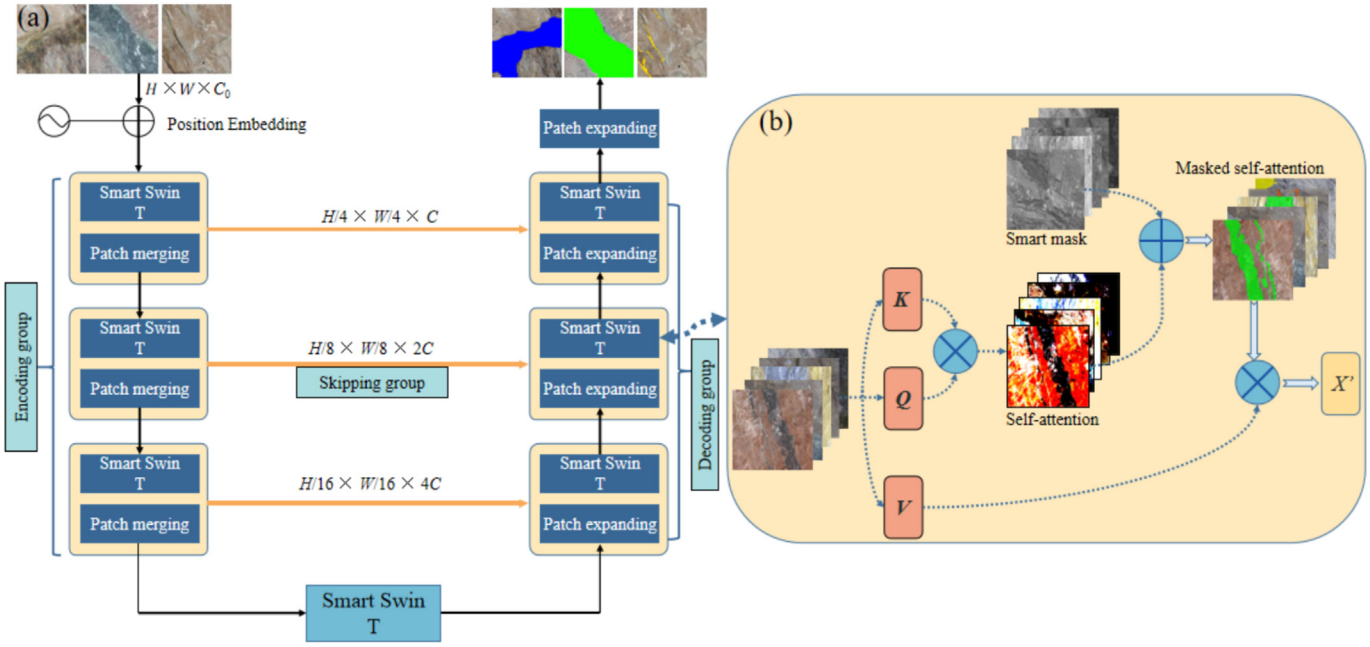

Fig. 3. Framework of (a) FRFseg model and (b) SSM-MSA module.

2.2 Bayesian network

BNs, alternatively referred to as belief networks or directed acyclic graphs, have garnered significant attention and research focus within geotechnical engineering for predictive tasks owing to their efficacy in managing incomplete datasets and uncertainty (Borsuk et al., 2004; Li et al., 2017a; Ou et al., 2022). BNs are graphical models utilized for illustrating dependencies among random variables. It employs a directed graph structure to depict inter-variable relationships and employs probability distributions for articulating these associations. Grounded in Bayesian theory, BNs offer a graphical representation that adeptly navigates issues of uncertainty and incomplete data, thereby finding extensive utility at the nexus of artificial intelligence and geotechnical engineering.

BNs generally consist of two components: nodes and edges. Nodes represent random variables, while edges denote dependencies between variables. The fundamental idea of BNs is to utilize conditional probabilities to depict the dependencies between nodes, thus constructing a comprehensive probability model. Assuming there exists a BN composed of random variables v_1, v_2,•••, v_n, its joint probability distribution can be expressed as

$$P(v_1, v_2, \cdots, v_n) = \sum \prod_{1}^{n} P(v_i|\mathrm{Pa}(v_i)), \tag{2}$$

where $P(v_i)$ signifies the ensemble of parental nodes associated with node v_i, and $P(v_i \mid \mathrm{Pa}(v_i))$ represents the conditional probability distribution of node v_i conditioned on its parental set.

The Naïve BN, depicted in Fig. 4(a), stands as the simplest and most commonly employed network, assuming conditional independence among all variables. However, in geotechnical engineering, many child nodes are often not entirely independent. For instance, in the probabilistic modeling of tunnel excavation processes, the rock type, construction method, and failure mode are frequently interrelated (Špačková & Straub, 2013). Likewise, when predicting underground cavern overbreak, correlations between joints, layer surfaces, and structural planes should not be disregarded (Gong et al., 2008). To address this, a tree-augmented naïve (TAN) BN is proposed, allowing for conditional relationships between variables (N. Li et al., 2017a). Its graphical structure is depicted in Fig. 4(b).

In practical engineering problems, the obstacle of incomplete data is frequently encountered. TAN BN methods exhibit advantages in achieving prediction tasks based on incomplete datasets, with the support of the Expectation-Maximization (EM) algorithm (Dempster, 1977; Feng & Jimenez, 2015). The EM algorithm encompasses multiple iterative steps.

Step 1: initialization step. The parameters of the BNs need to be set to their initial values. These parameters generally represent the conditional probabilities between nodes.

Step 2: expectation step (E-step). It is essential to compute the expectation of the missing variables based on the current parameter estimates. For each sample, calculate the probability of the sample belonging to a particular category. Let x be the observed variable, Z be the missing variable, and $E(x)$ be the current variable estimate. The objective of the E-step is to compute the expectation value

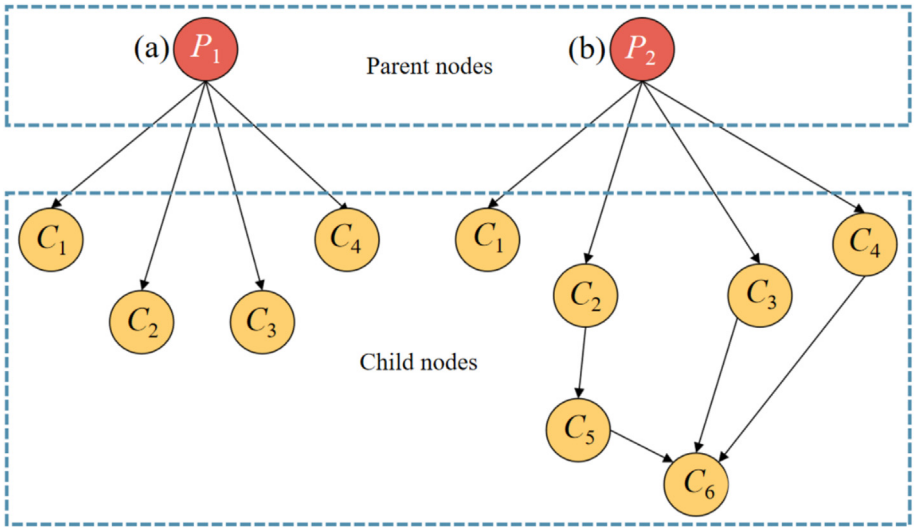

Fig. 4. Schematic diagram of (a) Naïve BN and (b) TAN BN.

of Z, which typically involves computing the expected value of conditional probabilities. The formula for expectation calculation is

$$Q(Z) = E\left[Z|x, \theta^{\text{old}}\right], \tag{3}$$

where $Q(Z)$ is the expectation of Z, and θ^{old} is the estimated parameter. Specifically, for each sample and each possible missing variable, the conditional probability $P(Z = z|x, \theta^{\text{old}})$ is calculated. Then, it is multiplied by Z, and finally, $Q(Z)$ is obtained by summing over all possible Z.

Step 3: maximization step (M-step). The lower bound of the log-likelihood function is maximized using the expected values of Z, thus updating the parameter estimates. The maximization formula is

$$\theta^{\text{new}} = \text{argmax\_}\theta\, Q\left(\theta|\theta^{\text{old}}\right), \tag{4}$$

where θ^{new} represents the updated parameter estimate, and argmax_θ Q refers to the parameter θ that maximizes the Q function.

Step 4: iterative step. Repeat E-step and M-step until the parameter estimates converge. The estimates from the previous iteration are utilized as the current values, and then E-step and M-step are executed to update the parameters. By iteratively performing the E-step and M-step, the EM algorithm gradually approaches the maximum likelihood estimate. In light of this, with the aid of the TAN BN in Netica software, the EM algorithm can be directly invoked.

3 Obtaining various parameter sets

In the domain of rock quality assessment, scholars often take into account parameters such as surface-apparent groundwater, fractures, internal borehole reference parameters during drilling, along with the rock physical–mechanical properties and design parameters. Nevertheless, the comparative predictive efficacy of these apparent, internal, physical–mechanical, and design parameter sets on rock quality has seldom been explored in conjunction. This work intends to construct distinct parameter sets derived from the aforementioned parameters, perform comparative analyses on their influence, and identify the optimal parameter set for evaluation.

3.1 Tunnel face apparent parameter set

3.1.1 Establishing tunnel face features image set

For the precise segmentation of rock features based on the FRFseg model, the establishment of a high-quality image dataset for training CV models is indispensable. To ensure the representativeness and transferability of this dataset, three tunnel projects characterized by distinct geomorphological and geological features are considered as sources of image samples. These projects include the Qingdao Jiaozhou Bay Second Submarine (QJSS) tunnel, the Yunnan Xuanhui Expressway (XHE) tunnel, and the Yunnan Mengping Expressway (MPE) tunnel. The QJSS tunnel spans approximately 17.5 km. Located within a coastal granite formation, the predominant rock types consist mainly of moderately to highly weathered granite and granite gneiss, influenced by various fault zones. The XHE tunnel extends over approximately 96.74 km, situated within the karstic terrain of the northeastern Yunnan Plateau. The route navigates a series of complex and unfavorable geological conditions. The MPE tunnel spans a total length of about 40.4 km, located in the southern Yunnan Plateau. Route maps, along with cross-sectional profiles representing the QJSS and XHE tunnels, are depicted in Fig. 5(a).

To establish an extensive database capturing the intricate details of rock features, an adaptive tunnel face image acquisition (ATIA) system is deployed. As illustrated in Fig. 5(b), the ATIA system comprises a Canon camera

Fig. 5. (a) Geographical location and route of various tunnels, and (b) schematic diagram of ATIA system.

mounted on a tripod, alongside a suite of measurement tools and equipment, including an illuminometer, laser rangefinder, thermo hygrometer, and two adjustable light sources. It is imperative to emphasize that during the image acquisition process, environmental variables such as temperature, humidity, lighting conditions, as well as the precise distance between the capture point and different sections of the tunnel face, are diligently recorded manually using the ATIA system. It is paramount to highlight the meticulous procedures involved in the image acquisition phase for tunnel faces. Subsequently, leveraging data from the three rock tunnels and the ATIA system, a comprehensive dataset comprising 2500 raw images depicting rock fractures, 3000 raw images illustrating groundwater presence, and 2500 raw images capturing weak interlayers is curated. However, these raw images are not directly utilized for the training of CV models. These images constitute a relatively small dataset. It is crucial to first understand the limitations imposed by small datasets on the performance of CV methods. The utilization of small training sets poses multifaceted constraints in the application, primarily stemming from DL models' heavy reliance on data volume and the inherent complexity of CV tasks. The following provides some aspects of these constraints: (1) limited model generalization capability; (2) insufficient robustness and training stability; (3) constrained model performance. Although the limitation imposed by small datasets poses a challenge, it can be addressed through several strategies. The solutions adopted in this work are as follows: Firstly, more rock images are collected from tunnel faces. Secondly, various transformations, such as rotation, scaling, cropping, and flipping, are applied to the existing preliminary data to enhance data diversity. Lastly, image generation techniques, specifically generative adversarial networks (GANs), are employed to produce new image samples based on the existing image set. By incorporating some random noise into the image generation process, GANs can, to a certain extent, enhance the generalization performance of the image set. Based on the aforementioned methods, 20 000 images are obtained for each of the features of interlayers, leakage, and fractures, totaling 60 000 rock feature images. Additionally, to investigate how the size of the training dataset affects the performance of CV methods, particularly for the more

sophisticated enhanced FRFseg method, 4000, 8000, 12 000, 16 000, and 20 000 images of each rock feature are selected for training. Additionally, key evaluation metrics such as Accuracy, Recall, F_1-score, and IoU are employed to comprehensively evaluate the performance of CV methods. Figure 6(a)–(b) illustrates the performance under these varying dataset conditions (with interlayers and leakage as examples). It is observable that as the size of the image set increases, the performance metrics of the CV model gradually improve. When the training dataset size is smallest, the model exhibits the worst performance across all metrics. The fastest improvement in evaluation metrics occurs between 4000 and 12 000 images. The best performance is achieved when the dataset size reaches 20 000 images. However, the rate of improvement slows down between 12 000 and 20 000 images. The above observations pertain to the impact of dataset sizes ranging from 4000 to 20 000 images on the performance of CV models. In the segmentation experiments conducted in this study, it was found that while increasing the number of images does enhance model performance when Accuracy exceeds 90%, the magnitude of this improvement is less significant compared to the improvement seen before Accuracy reaches 90%. Similar trends are observable in the curves of IoU, F_1-score, and Recall, as well as during the training processes of the Swin T, Deeplab V3+, and UNet. However, collecting excessive images poses significant disruptions and burdens on tunnel construction sites, construction engineers, and researchers. Therefore, balancing the number of images and the performance of CV models is also a task that strives to accomplish. Furthermore, exploring larger dataset sizes in the future is worthwhile, given sufficient time and cooperation from tunnel projects.

3.1.2 Segmentation via FRFseg model

The established rock image dataset is processed using an integrated workstation featuring 64 GB of RAM and an Intel Core i9-processor. To ensure the predictive effectiveness, several assumptions are adopted, as described below: (1) The feature distributions of the training data and testing data are identical. (2) The hidden layer structure of the model can effectively capture the latent features of the data. (3) The model architecture is sufficiently complex to fit the target of the problem. (4) The hardware resources are adequate to support the computational demands of model training.

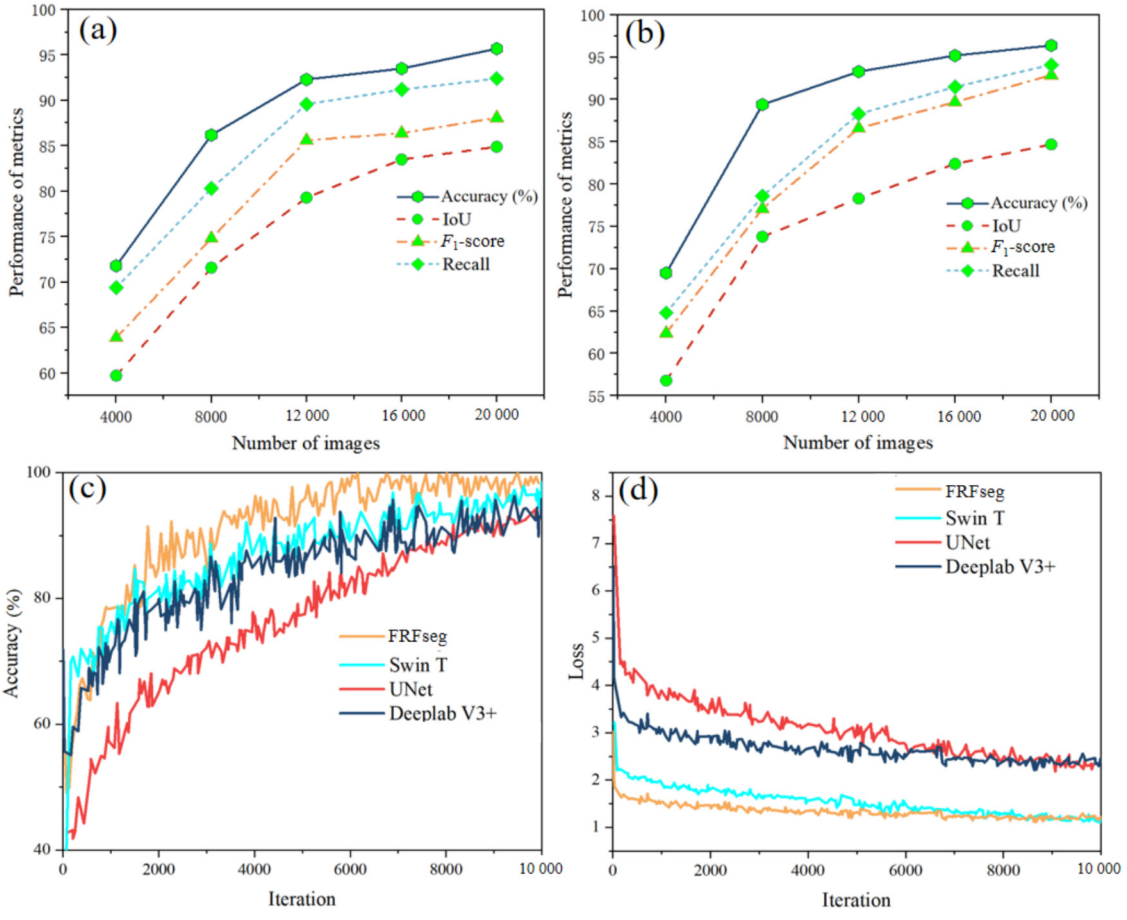

Fig. 6. Performance of different numbers of image sets. (a) Interlayers, (b) leakage, (c) Accuracy, and (d) Loss for various CV methods.

The current research applies comparative models, including the unmodified Swin T, Deeplab V3+, and UNet, to benchmark against state-of-the-art methods in the field. The Accuracy and Loss curves during the segmentation training process of the four models are depicted in Fig. 6 (c)–(d). It is evident from the results that, utilizing the rock image dataset, the segmentation accuracy of the FRFseg surpasses other comparative methods, with the fastest convergence rate observed in the improved method. These findings demonstrate the excellent performance of the improved model.

Figure 7 showcases the segmentation results of these models on various rock features. A detailed comparison of segmented outputs with marked images, particularly within highlighted areas, highlights the FRFseg model's superior accuracy in segmenting images with intricate boundaries and fine features. The FRFseg also demonstrates better continuity and integrity in its segmented outputs.

Following a comprehensive evaluation utilizing four metrics, the evaluation metrics of FRFseg consistently reside at the outermost perimeter of the radar chart (Fig. 8). The FRFseg method demonstrates markedly superior intelligent segmentation performance for weak interlayers, groundwater, and fractures compared to the other models. These results highlight the exceptional performance and capability of the FRFseg. During the testing process, it was found that the FRFseg method also outperforms several other Transformer-based methods, such as TransUNet (Chen et al., 2021b) and ST-UNet (He et al., 2022). The key factor contributing to its superiority is the SSW-MSA module. The core of its physical mechanism resides in the integration of the SSW-MSA module with self-attention matrices, which facilitates a more pronounced focus on the pertinent image information required. This includes crucial features such as interlayers, water leakage, and fractures on the tunnel face. Furthermore, through the utilization of an intelligent masking mechanism, the model effectively eliminates irrelevant information interactions while preserving accurate contextual data, thereby significantly enhancing its recognition capability for intricate detail features on the tunnel face. The synergistic effect of these physical mechanisms has led to a substantial improvement in the performance of the improved Swin T model for rock features. Moreover, the precise segmentation of these features ensures accurate parameter assessment for evaluating rock quality.

3.1.3 Establishing tunnel face apparent feature parameter set

In the evaluation process, readily observable features such as interlayers, leakage, and fractures are primary considerations, necessitating quantitative or qualitative recording (Barnard et al., 2016; Zhou et al., 2021). To establish a precise and efficient dataset of rock apparent parameters, it is essential to quantitatively process these rock features identified and segmented by the FRFseg model. As

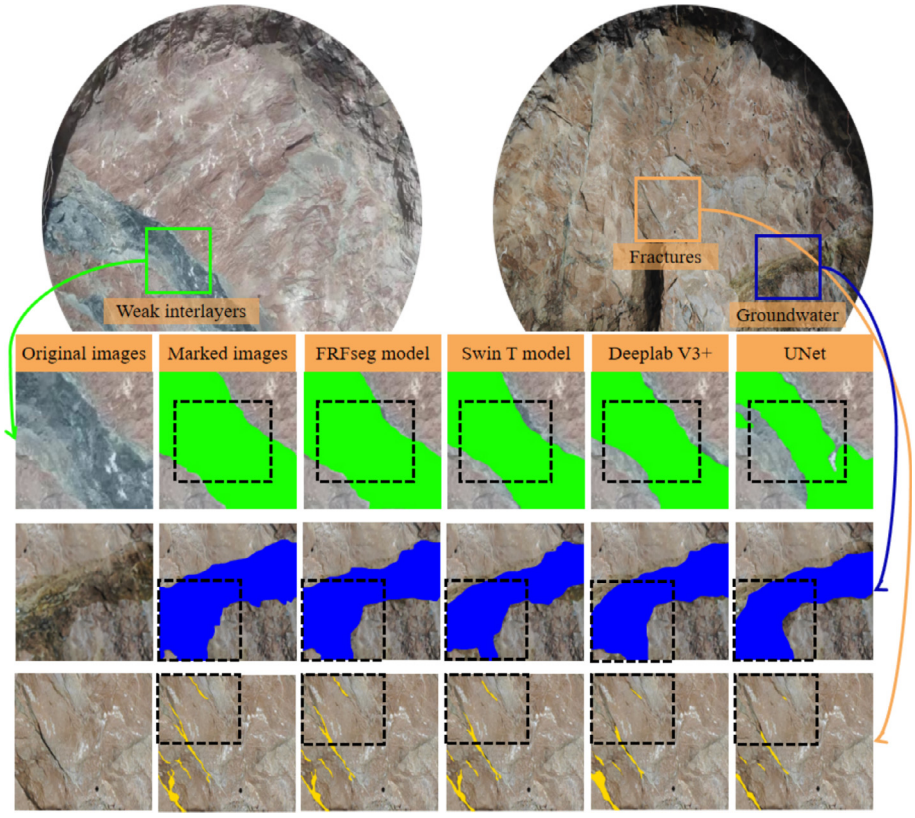

Fig. 7. Comparison of segmentation outcomes using various CV methods.

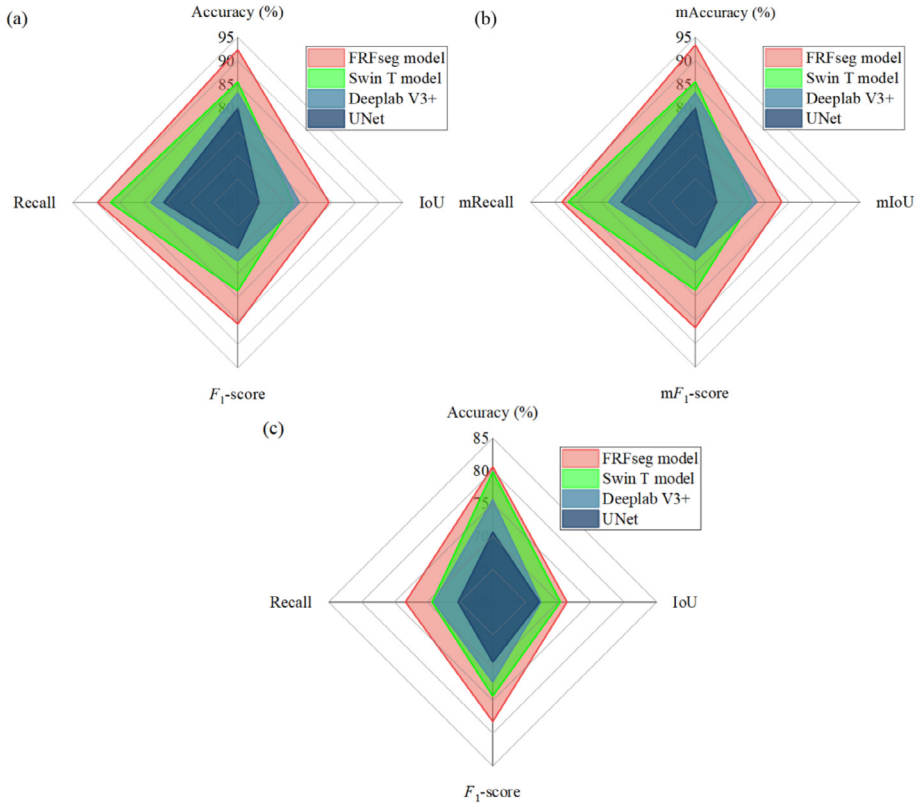

Fig. 8. Comparison of CV models for various metrics. (a) Interlayers, (b) leakage, and (c) fractures.

depicted in Table 1, the quantitative weak interlayer area (WIA), groundwater states (GWS), groundwater area, fracture trace number (FTN), maximum fracture trace length (MFTL), average fracture trace interval (AFTI), and fracture trace intensity (FTI) are employed in the designed tunnel face apparent feature (TFAF) parameter set. Due to space limitations, the detailed quantification method of these parameters is based on the segmented images, which can refer to our previous studies (Chen et al., 2020; Chen et al., 2021a; Wu et al., 2023).

3.2 Tunnel face internal features parameter set

Apart from the exhibition of apparent features, some internal drilling parameters such as drilling speed (DS), drilling speed stability (DSS), rotating pressure (RP), and drilling water state (DWS) have garnered attention from scholars (Chen & Yue, 2016; S. Li et al., 2017; Sugawara et al., 2003). Various studies have explored suitable drilling equipment and proposed methods for rock classification and quality prediction based on drilling parameters (S. Li et al., 2017; Yue et al., 2004). The drilling data employed is collected from advanced horizontal drilling operations conducted in the tunnel faces. As illustrated in Fig. 9(a), the drilling operations employed a three-arm rock drilling rig, specifically the ZT31Y integrated multi-function rock drilling rig, with a drill bit diameter of 76 mm. The horizontal drilling process is visualized in Fig. 9(b). Each tunnel face is subjected to drilling at five designated positions (as depicted in Fig. 9(c) for the drilling layout). Detailed drilling parameters utilized are outlined in Table 1.

3.3 Tunnel design and physical mechanics parameter set

It is meaningful to note that various rock physical and mechanical parameters, such as uniaxial compressive strength (UCS) and weathering degree (WD), as well as design parameters like tunnel design depth (TDD), exert considerable influence on rock quality. These parameters play a pivotal role in predicting (Huang et al., 2024; Zhou et al., 2021). Therefore, a tunnel design and physical mechanics (TDPM) set incorporating WD, UCS, and TDD is compiled for the analysis. The sources and introductions of the parameters in TDPM set are presented in Table 1.

3.4 Discretization of RQCE parameter set

To achieve a thorough and precise evaluation, a combined dataset comprising 14 parameters is designated as the rock quality comprehensive evaluate (RQCE) parameter set. This parameter set serves as a pivotal component in the assessment and characterization of rock masses. The basic information of the RQCE set is presented in Table 2.

Table 1
Various parameter sets for evaluating the rock quality.

Various dataset	Various parameter	Definition of parameter	Obtain source
TFAF	WIA	Area of interlayers depicted on tunnel face rock mass images	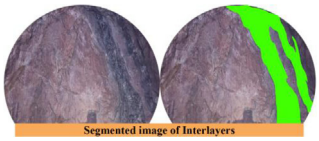
	GWS	Status of groundwater at tunnel faces: (1) Dry, (2) moist, (3) dripping, (4) flowing, and (5) surging (Wu et al., 2023)	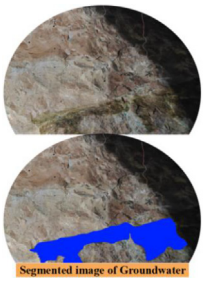
	GWA	Area of groundwater depicted on the tunnel face rock mass images	
	FTN	Number of fracture traces on the segmented image of the tunnel rock mass	
	MFTL	Maximal length of fracture traces depicted on rock mass segmented images	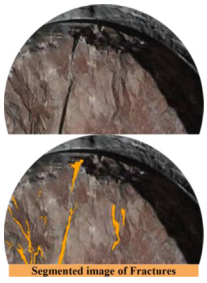
	AFTI	Average spacing of fracture traces on the rock mass	
	FTI	Fracture trace length within a unit window on the tunnel face rock mass	
TFIF	DS	Horizontal movement speed of advanced horizontal drilling in the rock mass	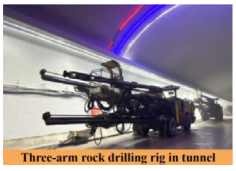
	DSS	Stability level of the horizontal movement speed of advanced horizontal drilling	
	RP	The force that drives the drill bit to rotate during horizontal drilling	
	DWS	Water output status of the borehole in the tunnel face rock mass	
TDPM	UCS	Uniaxial compressive strength of rocks, derived from in-situ point load tests conducted on rock samples obtained from the field	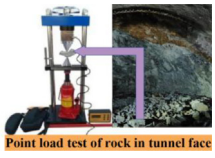
	WD	Rock weathering degree, obtained from the geological sketch data of the tunnel faces	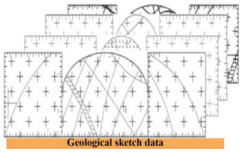
	TDD	Tunnel design depth of the working face	

Fig. 9. (a) T31Y integrated multi-function rock drilling rig, (b) horizontal drilling operation process, and (c) drilling layout diagram.

Table 2
Fundamental information of input and output parameters.

Various parameter		Number	Unit	Maximum value	Minimum value	Std. dev
Input	WIA	210	m^2	12.4	0	3.5
	GWS	210	–	4	1	1.1
	GWA	210	m^2	26.6	0	6.3
	FTN	76	–	22.5	2	4.7
	MFTL	118	m	1.89	0.2	0.5
	AFTI	75	m	0.71	0.05	0.2
	FTI	185	m	27.4	0	7.4
	DS	205	m/min	1.67	0.09	0.4
	DSS	208	–	3	1	0.59
	RP	202	bar	80	21	12.3
	DWS	211	L/min	120	0	26.1
	UCS	201	MPa	69.2	3.2	18.2
	WD	201	–	5	4	0.96
	TDD	116	m	381	11	91.3
Output	RMR	210	–	5	1	1.02

Theoretically, BN processing continuity and discrete data can be available, but BN has more advantages in processing discrete data and is more convenient for obtaining higher accuracy (Feng & Jimenez, 2015). To achieve an accurate evaluation, 11 continuous parameters in the RQCE set required discretization. Considering the predictive targets of this investigation and the RMR classification system as the reference scale, rock quality based on the RMR system is averaged and categorized into five levels. The continuous parameters in RQCE set are categorized into five levels. The specific discretization results are depicted in Fig. 10.

Furthermore, Table 2 displays the quantities, units, maximum values, and standard deviation (Std. dev) of 14 parameters. The calculation formula for Std. dev is described below.

$$X_{\text{Std.dev}} = \sum_{i=1}^{n} \frac{\sqrt{\Sigma(x_i - \bar{x})^2}}{n}, \tag{5}$$

where x_i is the i-th value of parameter X, and $\bar{x}$ is the average value of X. It is evident that not all parameters comprise 210 samples in Table 2. This indicates an incomplete data issue within the established parameter sets. To address this flaw, a TAN BN proficient in forecasting tasks with incomplete sets is considered and employed.

4 BN construction and evaluation

4.1 Establishment of BNs

To design the structure of TAN BN, it is first necessary to determine the correlation among the evaluation parameters. The correlation among the 14 parameters is demonstrated in Fig. 11. The darker color in this figure indicates the higher correlation between the two parameters. It can be seen that the absolute values of the correlation between DS and RP, DWS and GWS, GWS and GWA, FTN and AFTI, FTN and MFTL, FTN and TDD, AFTI and MFTL, as well as TDD and AFTI, are all greater than 0.6, indicating a strong correlation between them (N. Li et al., 2017a; Loozen et al., 2013). Based on the correlation results, a TAN BN structure is proposed (Fig. 12), where parameters with strong correlations have

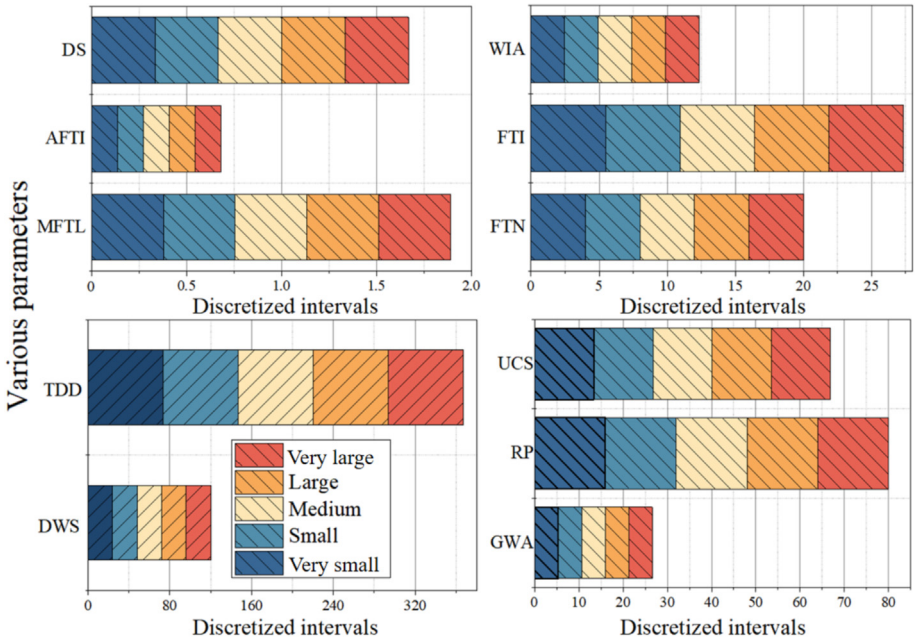

Fig. 10. Discretized intervals for different parameters.

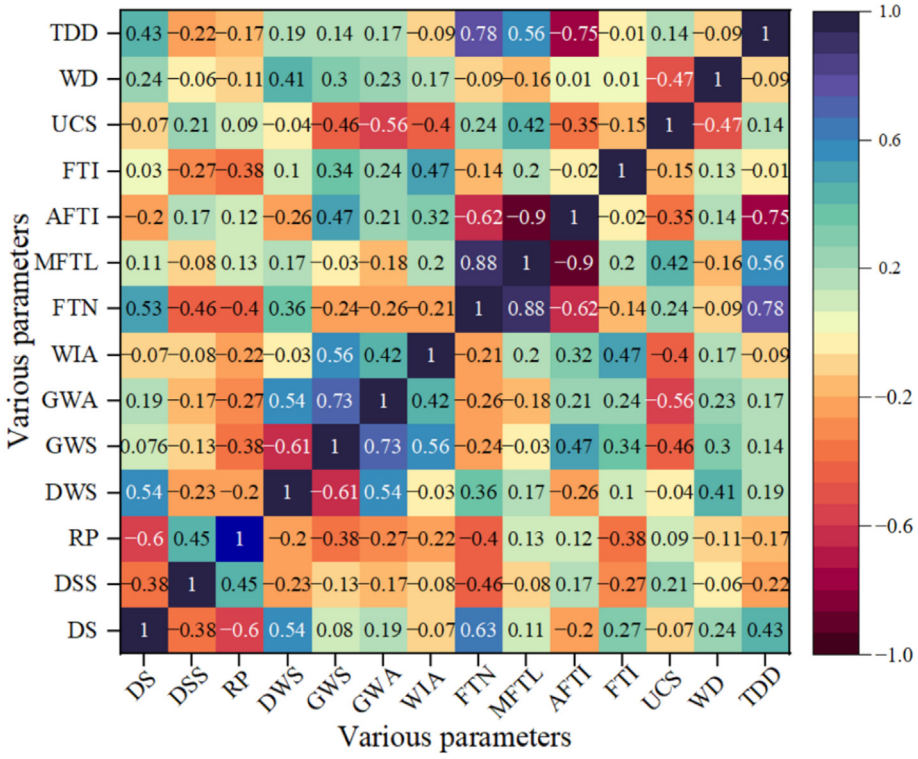

Fig. 11. Correlation analysis of 14 parameters.

been assigned new parent nodes (Feng & Jimenez, 2015; Liu et al., 2023).

4.2 Performance comparison of various datasets

To verify the effectiveness of the designed TAN BN, multiple pre-established multi-source parameter sets are employed for training and validation. These multi-source parameter sets are partitioned into training and validation sets in an 8:2 ratio. However, these multi-source parameter sets are characterized by incomplete data. To accurately evaluate rock quality based on these incomplete parameter sets, an EM algorithm is applied. In light of this, the EM algorithm and the TAN BN are applied to evaluation

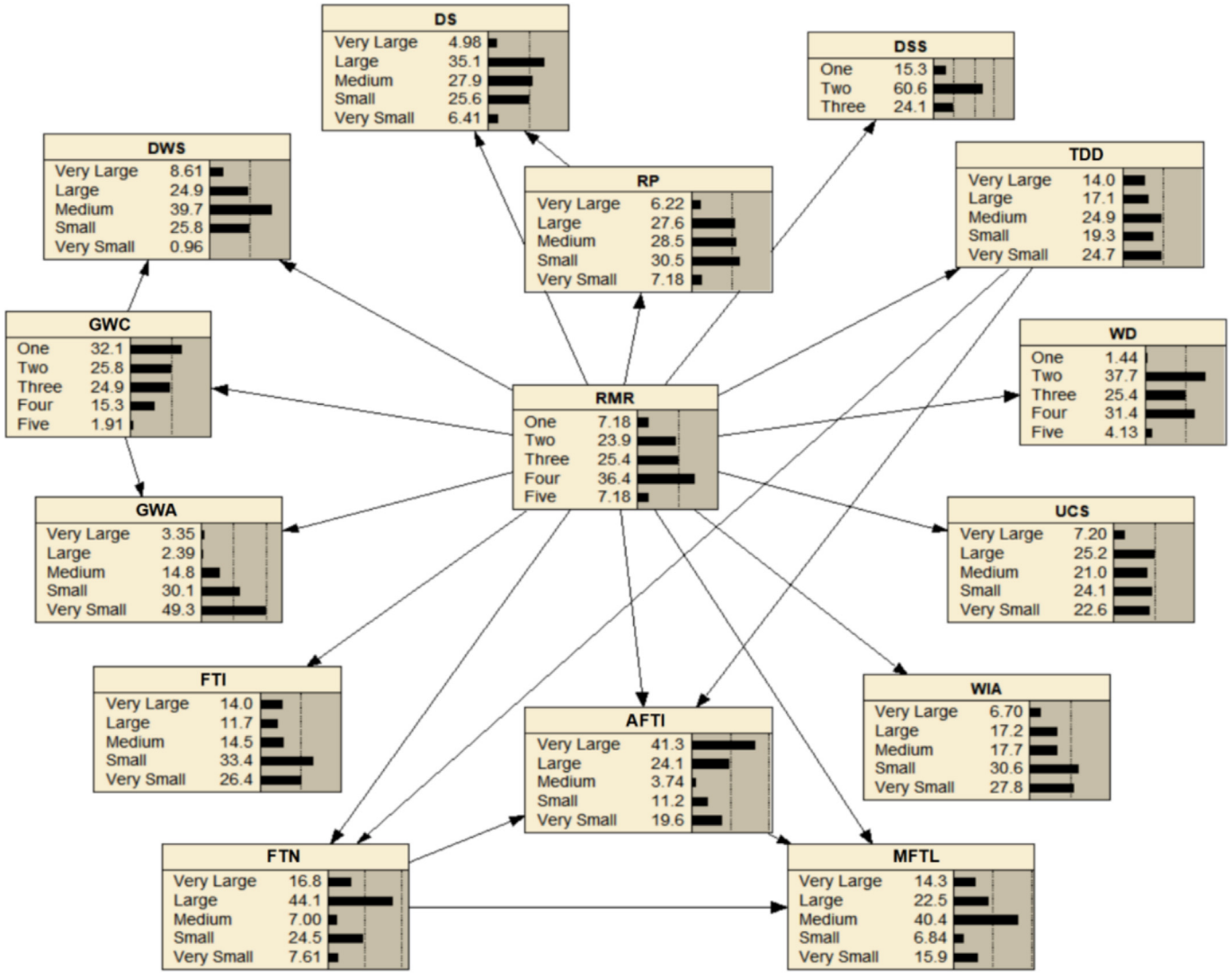

Fig. 12. Framework of the designed TAN BN.

based on various parameter sets with incomplete data, thereby determining the optimal parameter set. It should be noted that the established TFAF, tunnel face internal features (TFIF), TDPM, RQCE sets, and their combinations, such as TDPM + TFAF and TDPM + TFIF, are utilized for the training and validation of the TAN BN. The training and validation accuracies are illustrated in Fig. 13. It is evident that the RQCE set exhibits the best performance, while the TDPM set performs the poorest. Compared to the baseline TDPM set, the addition of TFIF parameters in TDPM + TFIF yields higher accuracy than TDPM + TFAF, highlighting the significant enhancement in accuracy through the inclusion of drilling parameters. Notably, the TFIF set achieves an accuracy of 83% using only four parameters, emphasizing the capacity of drilling parameters to more precisely reflect the true state of rock. Additionally, tunnel engineers have expressed keen interest in the non-contact safety approach based on TFAF, and have also taken into account the evaluation results provided by this intelligent and quick method.

Additionally, the training and validation accuracies achieved on the RQCE parameter set are 96% and 9.

Furthermore, the conditional probability table (CPT) is a fundamental component of BNs, encapsulating the dependencies among parameters. Specifically, each node's CPT delineates the conditional distribution of that parameter, given the values of its parent nodes. The CPT clearly elucidates the interdependencies between different nodes, indicating how the value of one node influences the values of other nodes. These dependencies are crucial in the learning and inference processes of BNs. Figure 15 illustrates the conditional probabilities of four representative parameters—WIA, FTI, RP, and WD. Using the CPT depicted in Fig. 15, one can perform inference, calculating the posterior probabilities of other nodes based on the observed values of known nodes. This inference process allows for the prediction of unknown nodes. For instance, when only the WIA is observed and its state is very small, there is a 93% confidence level in predicting as Level I. Similarly, when only the RP is observed and its state is very large,

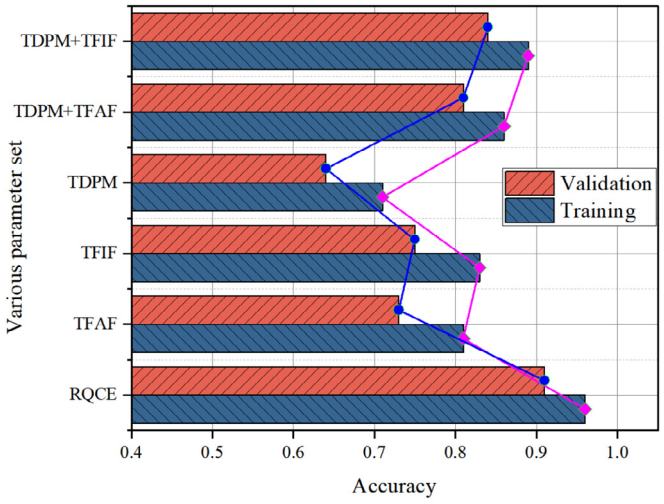

Fig. 13. Performance comparison of different parameter sets.

there is an 87% confidence level in evaluating the rock quality as Level I.

4.3 Case testing and comparisons with existing data-driven methods

The research conducted herein designs a TAN BN to support tunnel safety and excavation planning. To verify its robustness and generalizability, the TAN BN is evaluated on 70 recently excavated tunnel faces. The BN provides predictive and evaluative services regarding rock quality for these tunnel faces. Untrained data from these excavations are utilized to test the TAN BN's performance. Test results are visualized in confusion matrices (Fig. 14 (b)), demonstrating an average accuracy of 91%.

In the domain of geotechnical engineering for evaluation and classification, ML and DL methods are currently a focal point of application (Feng et al., 2021; Zhou et al., 2021). Commonly employed approaches encompass Naïve BN, decision tree models exemplified by classification and regression tree (CART), hybrid learning models such as gradient boosting regression tree (GBRT), artificial neural networks typified by MLP, as well as popular DL models, represented by deep neural network (DNN), are utilized as comparative references (Baghbani et al., 2022; Huang et al., 2022; Mohammadi et al., 2015). Through comprehensive comparison and assessment, insights into the advantages and limitations of TAN BN for specific tasks can be gleaned, aiding in the selection of the most suitable method for practical implementation. To evaluate the effectiveness of the designed TAN BN, evaluations for rock quality are juxtaposed across various methods, as illustrated in Fig. 16. Meanwhile, hyperparameter optimization was conducted for comparative models, and their optimal hyperparameter configurations are presented in Table 3. During the training and test phase, it is determined that TAN BN exhibits superior accuracy compared to other candidate models. This underscores the benefit of TAN BN's tree structure in capturing inherent patterns within the RQCE set. This observation highlights the superior accuracy of the TAN BN in newly encountered tunnel faces. Additionally, TAN BN exhibits enhanced transferability and adaptability.

5 Bayesian updates and sensitivity analysis

Bayesian updating, a statistical technique grounded in Bayes' theorem, allows for the step-by-step revision of probability estimates for a specific event as new data is introduced. This methodology is especially crucial in ML and artificial intelligence, where it facilitates models in refining their internal probability distributions based on newly acquired data (Lauritzen & Spiegelhalter, 1988; N. Li et al., 2017b). The core formula of Bayesian updating is expressed as follows:

$$P(A|B) = (P(B|A) \times P(A)) / P(B), \tag{6}$$

where $P(A|B)$ denotes the conditional probability of A given B, referred to as the posterior probability. This represents the updated probability estimate of A. $P(A)$ signifies the prior probability of A. By applying Bayesian updating, $P(A)$ and $P(B|A)$ are combined to refine the TAN BN's probability estimates for rock quality with new information. This updating mechanism allows the designed BN to effectively handle uncertainties. Section 4.3 is designated

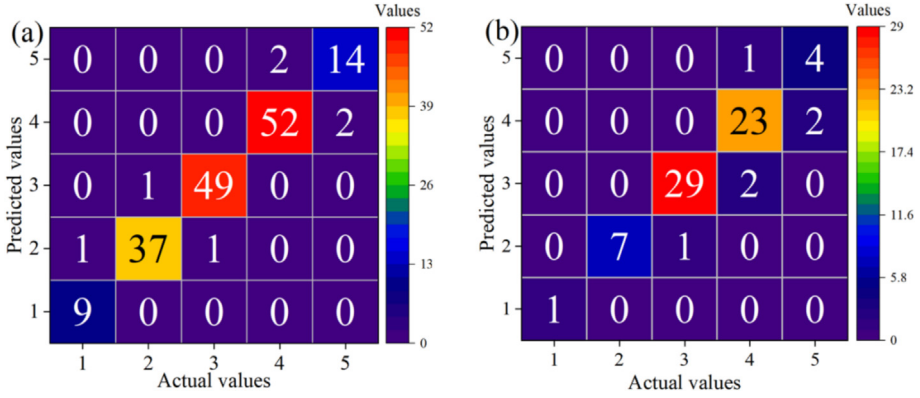

Fig. 14. Evaluation results of rock quality based on designed TAN BN: (a) training, and (b) test process.

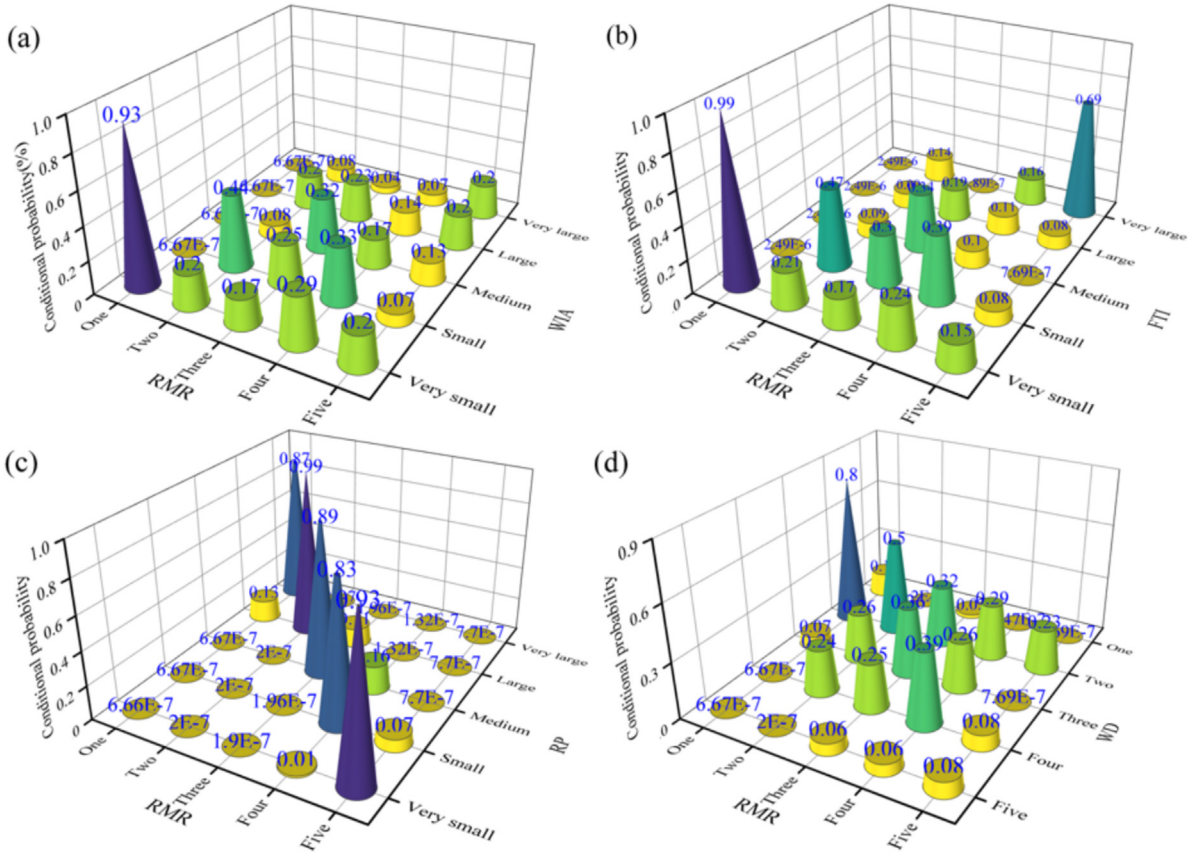

Fig. 15. Conditional probabilities of various parameters and rock quality.

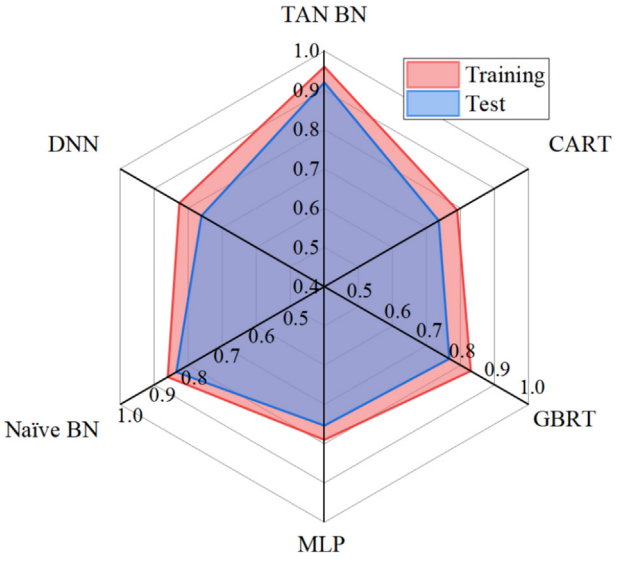

Fig. 16. Comparison of performance for various methods.

as the BN updating section. Moreover, the updated TAN BN facilitates the visual classification and probabilistic evaluation of rock quality. For example, as depicted in Fig. 17(a), when WIA = Medium, GWS = Two, and other conditions, the rock quality is evaluated as Level IV, with a conditional probability of 57.2%.

For sensitivity evaluation, mutual information (MI) and variance reduction (VR) are frequently utilized metrics, extensively applied to evaluate various underground engineering problems (N. Li et al., 2017b). These metrics are instrumental in identifying key input parameters that substantially impact the model's output, facilitating model optimization and decision-making processes. MI metric quantifies the interactions and dependencies among distinct input parameters and the output within a parameter set. The VR serves as a metric to assess the impact extent of model input on output variance. VR metric is often regarded as the reduction in the variance of U due to the appearance of x. When the VR calculation results are 0, it indicates that there is no correlation between the input and output parameters.

The results of MI and VR metrics, calculated for 14 parameters, are depicted in Fig. 18. Particularly, RP, DS, and FTN emerge as the top three parameters exerting the most substantial influence on rock quality, which is consistent with the observations made in the tunnels providing quality prediction services. Tunnel site engineers have more confidence in evaluating the quality based on parameters obtained from advanced prediction operations such as RP and DS. This increased confidence may be attributed to the fact that RP represents the necessary force to overcome rock strength and fracture the rock mass. Higher rock strength, integrity, and stability require proportion-

Table 3
Hyperparameter settings for various models.

Algorithm	Hyper-parameter	Searching space	Optimal value
CART	*N* estimators	[20, 200]	95
	Max features	[1, 10]	5
GBRT	*N* estimators	100, 300	230
	Max depth	1, 15	6
	Min samples split	1, 15	13
	Learning rate	1×10^{-3}, 5×10^{-1}	0.9
	Max features	1, 10	7
	Subsample	5×10^{-1}, 1	0.92
MLP	Alpha	$e \times 10^{-5}$, 1×10^{-2}	0.0016
	Momentum	0, 1	0.14
	Learning rate	Constant, invscaling, adaptive	Adaptive
	Activation	Tanh, ReLU	Tanh
	Init learning rate	1×10^{-3}, 5×10^{-1}	0.18
DNN	Hidden_layers	[10, 16]	12
	Hidden_size	[15, 25]	20
	Learning_rate	[1×10^{-4}, 1×10^{-2}]	0.007
	Dropout	[0.1, 0.5]	0.13

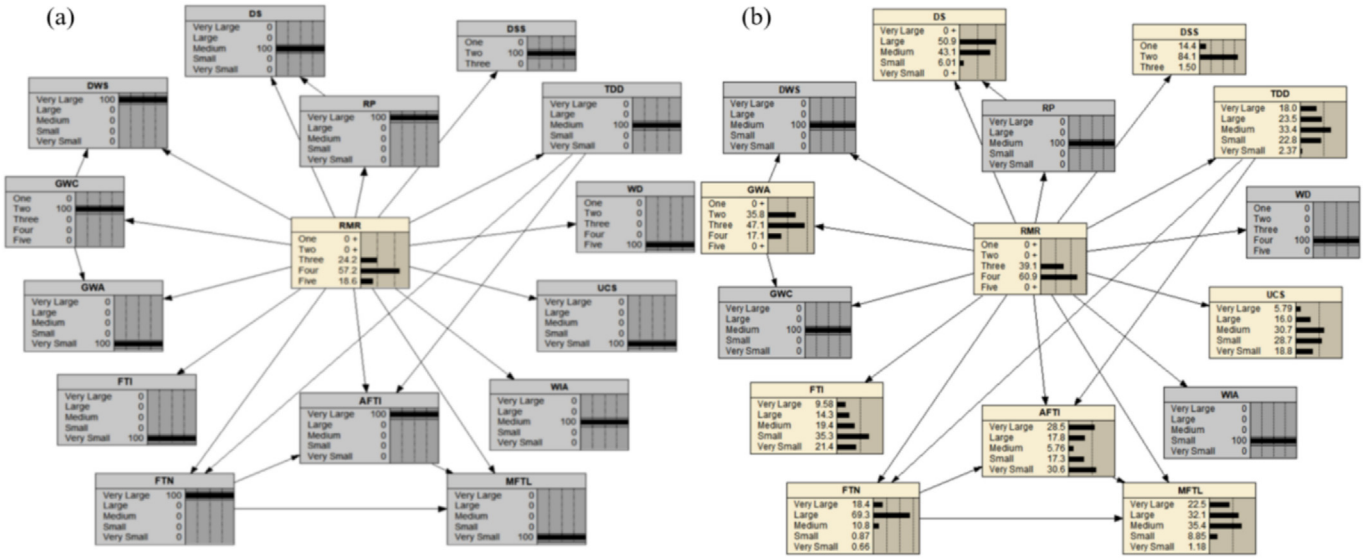

Fig. 17. (a) TAN BN of specific working conditions, and (b) TAN BN of obtaining partial parameters.

ately higher RP, whereas lower strength and stability necessitate reduced RP. Consequently, analyzing rotating pressure provides a reliable parameter of rock quality. DS ranks as the second most impactful parameter, attributed to factors like rock strength, weathering state, and fracture development, which directly affect drilling difficulty. Harder, less weathered, and fissure-reduced rock demands more energy and time to break apart, resulting in slower DS. Conversely, rocks exhibiting opposite characteristics enable faster drilling. Therefore, DS offers a direct insight into the internal state of rock mass (Kalantari et al., 2019, 2018).

6 Discussion

It is noteworthy that a limitation of this study lies in the challenge of recording Level I rock mass at the tunnel excavation sites within the tunnels providing rock quality assessment services, due to the adverse geological conditions such as karst strata, soft rock, and the influence of groundwater and weak interlayer. Consequently, the dataset is predominantly focused on rock grades ranging from Level II to Level V, with limited data on Level I. Future efforts will aim to address this limitation by collecting

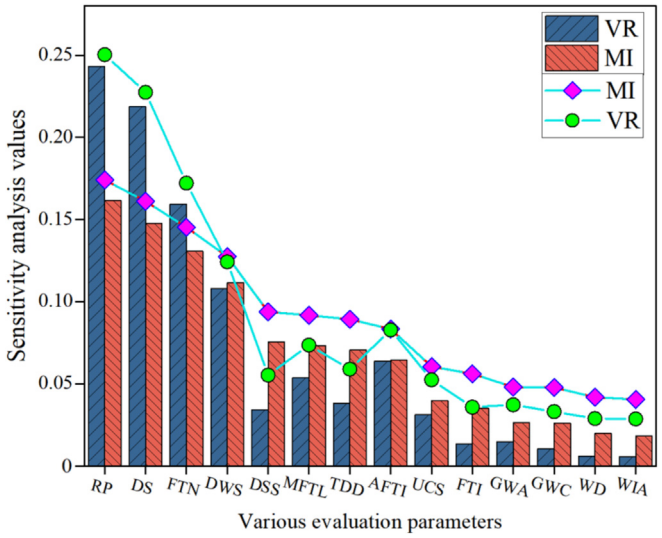

Fig. 18. Assessment of importance for various parameters.

comprehensive RMR data to expand the predictive capabilities of the designed BN.

In tunnel engineering assessment tasks, the performance of DL models often surpasses ML models in most cases. However, the TAN BN is designed based on the rock quality comprehensive evaluation set, which integrates apparent, internal, rock physical–mechanical, and design parameters, and achieves a more satisfactory evaluation performance than DL methods. This superiority can be attributed to the higher complexity of DL models, which typically require a significant amount of data for training. On small datasets, where data availability is limited, DL may fail to fully capture the inherent patterns and characteristics of the data, resulting in poor model generalization and inferior performance compared to ML models. Moreover, DL methods are more prone to overfitting on small datasets. Collecting a large amount of tunnel data to achieve satisfactory performance for DL often imposes a significant burden on tunnel engineers. Therefore, the implementation of the easily interpretable TAN BN with a relatively small dataset to achieve a more satisfying evaluation effect for engineers than DL is worth exploring.

Moreover, the cost-effectiveness and feasibility of the proposed method deserve attention. The method possesses the capability to carry out prediction tasks even when only partial evaluation parameters are obtained. The most expensive parameter to collect is the drilling parameter. For some large-scale projects with budget constraints, some evaluation parameters in the TAN BN can be selectively collected within the allowed cost range, while those with excessively high costs can be omitted, thereby proceeding with the prediction and providing corresponding confidence levels. This will enhance the cost-effectiveness and feasibility of the proposed method in these projects. To reduce the complexity of the proposed method, selecting a certain number of parameters is recommended for different tunnel projects based on their geological characteristics, costs, and construction schedules, thereby facilitating the prediction of surrounding rock quality. As depicted in Fig. 17(b), this paper utilizes the TAN BN constructed using Netica software, which allows for the prediction using a subset of parameters provided by the project, without imposing excessive burdens on the project. Additionally, it is recommended that project personnel utilize Netica software to operate the TAN BN. Netica is a user-friendly and interactive software with a compact size. Operators on tunnel projects do not need to delve deeply into the mathematical and software backgrounds; instead, they can simply click on the pre-established TAN BN within Netica to achieve predictions. Thus, the complexity of the underlying mathematics does not hinder the application of the method proposed.

7 Conclusions

The following conclusions can be drawn from this study.

(1) Drawing from the basic structures of the Swin T and UNet, a smart FRFseg model is employed. Its U-shaped architecture and smart W-MSA significantly enhance its ability to segment rock features. The segmentation experiments of fractures, groundwater, and weak interlayers are carried out and compared with the common methods. FRFseg model yields the most superior segmentation results, suggesting promising avenues for refining CV methods based on rock specific characteristics.
(2) Six parameter sets are established, comprising apparent rock parameters obtained through CV methods, internal parameters, as well as design and physical–mechanical parameters, totaling 14 parameters. The findings confirm that the rock quality comprehensive evaluation set achieves the highest accuracy, reaching 91%. Further, the study underscores the critical role of drilling parameters.
(3) Addressing the inherent data incompleteness in the rock quality comprehensive evaluation dataset, a novel tree-structured TAN BN is designed. A comparative analysis against popular ML and DL methods reveals TAN BN's superior predictive accuracy, especially in managing incomplete datasets. Sensitivity analysis further identifies parameters significantly impacting the evaluation, emphasizing the importance of RP and the minimal influence of WIA parameter.

Data availability

The data employed to drive the TAN BN can be obtained from the following link: Https://github.com/BluesOctopus/

Data-driven-Bayesian-networks-Data-V1-.git. And the code of the applied visual method is as follows: https://github.com/suofer/Smart-Swin-Transforme.

CRediT authorship contribution statement

Chen Wu: Writing – review & editing, Writing – original draft, Formal analysis, Methodology, Software. **Minglun Tan:** Funding acquisition, Project administration, Data curation. **Yue Tong:** Funding acquisition, Data curation. **Hongwei Huang:** Writing – review & editing, Project administration, Formal analysis, Supervision, Funding acquisition, Conceptualization.

Declaration of competing interest

The authors declare that they have no known competing financial interests or personal relationships that could have appeared to influence the work reported in this paper.

Acknowledgement

The work described in this paper is supported by the National Natural Science Foundation of China (Grant No. 52279107), Qingdao Guoxin Jiaozhou Bay Second Submarine Tunnel Co., Ltd., Academician and Expert Workstation of Yunnan Province (Grant No. 202205AF150015), and the Science and Technology Innovation Project of YCIC Group Co., Ltd. (Grant No. YCIC-YF-2022-15)

References

Baghbani, A., Choudhury, T., Costa, S., & Reiner, J. (2022). Application of artificial intelligence in geotechnical engineering: A state-of-the-art review. *Earth-Science Reviews, 228*, 103991.

Barnard, C., Kallu Raj, R., Warren, S., & Thareja, R. (2016). Inflatable rock bolt bond strength versus rock mass rating (RMR): A comparative analysis of pull-out testing data from underground mines in Nevada. *International Journal of Mining Science and Technology, 26*(1), 19–22.

Barton, N., Lien, R., & Lunde, J. (1974). Engineering classification of rock masses for the design of tunnel support. *Rock Mechanics and Rock Engineering, 6*(4), 189–236.

Borsuk, M. E., Stow, C. A., & Reckhow, K. H. (2004). A Bayesian network of eutrophication models for synthesis, prediction, and uncertainty analysis. *Ecological Modelling, 173*(2/3), 219–239.

Chen, C. S., & Liu, Y. C. (2007). A methodology for evaluation and classification of rock mass quality on tunnel engineering. *Tunnelling and Underground Space Technology, 22*(4), 377–387.

Chen, J., & Yue, Z. Q. (2016). Weak zone characterization using full drilling analysis of rotary-percussive instrumented drilling. *International Journal of Rock Mechanics and Mining Sciences, 89*, 227–234.

Chen, J. Q., Li, X. J., Zhu, H. H., & Rubin, Y. (2017). Geostatistical method for inferring RMR ahead of tunnel face excavation using dynamically exposed geological information. *Engineering Geology, 228*, 214–223.

Chen, J. Y., Huang, H. W., Cohn, A. G., Zhang, D. M., & Zhou, M. L. (2022). Machine learning-based classification of rock discontinuity trace: SMOTE oversampling integrated with GBT ensemble learning. *International Journal of Mining Science and Technology, 32*(2), 309–322.

Chen, J. Y., Zhang, D. M., Huang, H. W., Shadabfar, M., Zhou, M. L., & Yang, T. J. (2020). Image-based segmentation and quantification of weak interlayers in rock tunnel face via deep learning. *Automation in Construction, 120*, 103371.

Chen, J. Y., Zhou, M. L., Huang, H. W., Zhang, D. M., & Peng, Z. C. (2021a). Automated extraction and evaluation of fracture trace maps from rock tunnel face images via deep learning. *International Journal of Rock Mechanics and Mining Sciences, 142*, 104745.

Chen, J.N., Lu Y.Y, & Yu, Q. H. (2021b). TransUNet: transformers make strong encoders for medical image segmentation. https://arxiv.org/abs/2102.04306v1.

Dempster, A. P. (1977). Maximum likelihood from incomplete data via the EM algorithm. *Journal of the Royal Statistical Society, 39*(1), 1–22.

Feng, S. X., Chen, Z. Y., Luo, H., Wang, S. Y., Zhao, Y. F., Liu, L. P., Ling, D. S., & Jing, L. J. (2021). Tunnel boring machines (TBM) performance prediction: A case study using big data and deep learning. *Tunnelling and Underground Space Technology, 110*, 103636.

Feng, X. D., & Jimenez, R. (2015). Predicting tunnel squeezing with incomplete data using Bayesian networks. *Engineering Geology, 195*, 214–224.

Fu, L. Y., Chen, Y. Z., Ji, W., & Yang, F. (2024). SSTrans-Net: Smart swin transformer network for medical image segmentation. *Biomedical Signal Processing and Control, 91*, 106071.

Gong, F. Q., Li, X. B., & Zhang, W. (2008). Over-excavation forecast of underground opening by using Bayes discriminant analysis method. *Journal of Central South University of Technology, 15*(4), 498–502.

Guo, P., Bu, M., Zhang, P., Li, Q., & He, M. (2023). Review on catastrophe mechanism and disaster countermeasure of high geotemperature tunnels. *Chinese Journal of Rock Mechanics and Engineering, 42*, 1561–1581 (in Chinese).

He, X., Zhou, Y., & Zhao, J. (2022). Swin transformer embedding UNet for remote sensing image semantic segmentation. *IEEE Transactions on Geoscience and Remote Sensing, 60*, 4408715.

Hou, S., Liu, Y., & Yang, Q. (2022). Real-time prediction of rock mass classification based on TBM operation big data and stacking technique of ensemble learning. *Journal of Rock Mechanics and Geotechnical Engineering, 14*(1), 123–143.

Huang, H., Wu, C., Zhou, M., Chen, J., Han, T., & Zhang, L. (2024). Rock mass quality prediction on tunnel faces with incomplete multi-source dataset via tree-augmented naive Bayesian network. *International Journal of Mining Science and Technology, 34*(3), 323–337.

Huang, M. Q., Ninic, J., & Zhang, Q. B. (2021). BIM, machine learning and computer vision techniques in underground construction: Current status and future perspectives. *Tunnelling and Underground Space Technology, 108*, 103677.

Huang, Z., Liao, M. X., Zhang, H. L., Zhang, J. B., Ma, S. K., & Zhu, Q. X. (2022). Predicting tunnel squeezing using the SVM-BP combination model. *Geotechnical and Geological Engineering, 40*, 1387–1405.

Ismail, M. A. M., Majid, T. A., Goh, C. O., Lim, S. P., & Tan, C. G. (2019). Geological assessment for tunnel excavation under river with shallow overburden using surface site investigation data and electrical resistivity tomography. *Measurement, 144*, 260–274.

Kalantari, S., Baghbanan, A., & Hashemalhosseini, H. (2019). An analytical model for estimating rock strength parameters from small-scale drilling data. *Journal of Rock Mechanics and Geotechnical Engineering, 11*(1), 135–145.

Kalantari, S., Hashemolhosseini, H., & Baghbanan, A. (2018). Estimating rock strength parameters using drilling data. *International Journal of Rock Mechanics and Mining Sciences, 104*, 45–52.

Lauritzen, S. L., & Spiegelhalter, D. J. (1988). Local computations with probabilities on graphical structures and their application to expert systems. *Journal of the Royal Statistical Society: Series B (Methodological), 50*(2), 157–194.

Li, N., Feng, X., & Jimenez, R. (2017a). Predicting rock burst hazard with incomplete data using Bayesian networks. *Tunnelling and Underground Space Technology Incorporating Trenchless Technology Research, 61*, 61–70.

Li, N., Jimenez, R., & Feng, X. D. (2017b). The influence of bayesian networks structure on rock burst hazard prediction with incomplete data. In *ISRM European Rock Mechanics Symposium (EUROCK)* (pp. 206–214). Ostrava: The Czech Republic.

Li, S. C., Liu, B., Xu, X. J., Nie, L. C., Liu, Z. Y., Song, J., Sun, H. F., Chen, L., & Fan, K. R. (2017c). An overview of ahead geological prospecting in tunneling. *Tunnelling and Underground Space Technology, 63*, 69–94.

Lin, A. L., Chen, B. Z., Xu, J. Y., Zhang, Z., Lu, G. M., & Zhang, D. (2022). DS-TransUNet: Dual swin transformer U-net for medical

image segmentation. *IEEE Transactions on Instrumentation and Measurement, 71*, 4005615.

Liu, W. L., Shao, Y. X., Li, C., Li, C. Q., & Jiang, Z. H. (2023). Development of a non-Gaussian copula Bayesian network for safety assessment of metro tunnel maintenance. *Reliability Engineering & System Safety, 238*, 109423.

Liu, Z., Lin, Y. T., Cao, Y., Hu, H., Wei, Y. X., Zhang, Z., Lin, S., & Guo, B. N. (2021). Swin transformer: Hierarchical vision transformer using shifted windows. In *Proceedings of the 18th IEEE/CVF International Conference on Computer Vision (ICCV), IEEE Network* (pp. 9992–10002).

Loozen, G., Ozcelik, O., Boon, N., De Mol, A., Schoen, C., Quirynen, M., & Teughels, W. (2013). Inter-bacterial correlations in subgingival biofilms: A large-scale survey. *Journal of Clinical Periodontology, 41*(1), 1–10.

Mohammadi, S. D., Naseri, F., & Alipoor, S. (2015). Development of artificial neural networks and multiple regression models for the NATM tunnelling-induced settlement in Niayesh subway tunnel, Tehran. *Bulletin of Engineering Geology and the Environment, 74*(3), 827–843.

Ou, X. D., Wu, Y. F., Wu, B., Jiang, J., & Qiu, W. X. (2022). Dynamic Bayesian network for predicting tunnel-collapse risk in the case of incomplete data. *Journal of Performance of Constructed Facilities, 36*(4), 04022034.

Palmstrom, A. (1996). Characterizing rock masses by the RMi for use in practical rock engineering: Part 1: The development of the Rock Mass index (RMi). *Tunnelling and Underground Space Technology, 11*(2), 175–188.

Patel, A. K., & Chatterjee, S. (2016). Computer vision-based limestone rock-type classification using probabilistic neural network. *Geoscience Frontiers, 7*(1), 53–60.

Qin, S. J., Qi, T. Y., Deng, T., & Huang, X. D. (2024). Image segmentation using Vision Transformer for tunnel defect assessment. *Computer-Aided Civil and Infrastructure Engineering, 39*(21), 3243–3268.

Špačková, O., & Straub, D. (2013). Dynamic Bayesian network for probabilistic modeling of tunnel excavation processes. *Computer-Aided Civil and Infrastructure Engineering, 28*(1), 1–21.

Sugawara, J., Yue, Z. Q., Tham, L. G., Law, K. T., & Lee, C. F. (2003). Weathered rock characterization using drilling parameters. *Canadian Geotechnical Journal, 40*(3), 661–668.

Tu, W. F., Li, L. P., Li, S. C., Shi, S. S., Zhou, Z. Q., & Chen, D. Y. (2019). Research on the application of dynamic weighting on the rock mass quality rating. *Arabian Journal of Geosciences, 12*(3), 87.

Wang, Q., Gao, H. K., Jiang, B., Li, S. C., He, M. C., & Qin, Q. (2021). In-situ test and bolt-grouting design evaluation method of underground engineering based on digital drilling. *International Journal of Rock Mechanics and Mining Sciences, 138*, 104575.

Wu, C., Huang, H. W., Zhang, L., Chen, J. Y., Tong, Y., & Zhou, M. L. (2023). Towards automated 3D evaluation of water leakage on a tunnel face via improved GAN and self-attention DL model. *Tunnelling and Underground Space Technology, 142*, 105423.

Yue, Z. Q., Lee, C. F., Law, K. T., & Tham, L. G. (2004). Automatic monitoring of rotary-percussive drilling for ground characterization—illustrated by a case example in Hong Kong. *International Journal of Rock Mechanics and Mining Sciences, 41*(4), 573–612.

Zhou, M., Chen, J., Huang, H., Zhang, D., Zhao, S., & Shadabfar, M. (2021). Multi-source data driven method for assessing the rock mass quality of a NATM tunnel face via hybrid ensemble learning models. *International Journal of Rock Mechanics and Mining Sciences, 147*, 104914.

Zhou, Z., Zhang, J. J., & Gong, C. J. (2023). Hybrid semantic segmentation for tunnel lining cracks based on Swin Transformer and convolutional neural network. *Computer-Aided Civil and Infrastructure Engineering, 38*(17), 2491–2510.